

## Nonmesonic Decay of Helium Hyperfragments

H. G. MILLER,\* M. W. HOLLAND, J. P. ROALSVIG, AND R. G. SORENSEN

*Department of Physics and Astronomy, State University of New York, Buffalo, New York*

(Received 8 November 1967)

Approximately 35 000  $K^-$  capture stars in an emulsion stack were examined for hyperfragments. A sample of  $\pi^-$ -mesonic and nonmesonic He hyperfragments was selected for the purpose of estimating the nonmesonic-to- $\pi^-$ -mesonic decay ratios for  ${}_{\Lambda}\text{He}$  and for  ${}_{\Lambda}\text{He}^5$ . The following values were obtained:  $Q({}_{\Lambda}\text{He}) = 1.02 \pm 0.15$ ,  $Q({}_{\Lambda}\text{He}^5) = 1.21 \pm 0.19$ , for the nonmesonic-to- $\pi^-$  mesonic decay ratios of  ${}_{\Lambda}\text{He}$  and  ${}_{\Lambda}\text{He}^5$ , respectively. Also, an attempt was made to estimate the ratio of proton stimulation to neutron stimulation for the nonmesonic decays of  ${}_{\Lambda}\text{He}$  and  ${}_{\Lambda}\text{He}^5$ , for various cutoff energies of the observed "fast protons." Furthermore, by combining our data with previous results, we obtained estimates of the nonmesonic and the total decay rates of  ${}_{\Lambda}\text{He}^4$  and  ${}_{\Lambda}\text{He}^6$ .

### I. INTRODUCTION

THE study of nonmesonic decays of hyperfragments has been limited by the difficulty in identifying the decaying hyperfragments. In the case of  ${}_{\Lambda}\text{He}$ , one must rely on determination of the charge of the hyperfragment by profile measurements. Previous experiments have attempted to measure the nonmesonic decay rate for  ${}_{\Lambda}\text{He}$  (see Table VII). The results have been limited by uncertainties in separating the charge two hyperfragments from the charge one events, including a large number of  $\Sigma^-$  capture events. In this experiment a good separation of charge two and charge one events has been achieved. In this paper, we discuss the results obtained from a study of the nonmesonic decays of  ${}_{\Lambda}\text{He}^{4,5}$ . In particular, an attempt has been made to determine the nonmesonic-to- $\pi^-$ -mesonic (or simply nonmesonic-to-mesonic) ratio and the ratio of proton to neutron stimulation for  ${}_{\Lambda}\text{He}^{4,5}$  and for  ${}_{\Lambda}\text{He}^5$  alone. In addition, the nonmesonic and total decay rates for  ${}_{\Lambda}\text{He}^4$  and  ${}_{\Lambda}\text{He}^5$  have been estimated.

### II. EXPERIMENTAL PROCEDURE

#### A. Scanning and Emulsion Stack Calibration

The scanning technique and the calibration of the emulsion stack have been described in a previous paper.<sup>1</sup> In both the previous and the present work, only the 45 interior pellicles from a stack of 100 KTB-5 emulsion pellicles (15 cm  $\times$  10 cm  $\times$  0.07 cm) were area scanned. Approximately 35 000  $K^-$ -capture stars (or primary stars) were observed and recorded.

The same range-energy calibration correction has again been used on all measurements made in the present work. Also, the range and angle measurements and the kinematic analysis of the mesonic decays of  ${}_{\Lambda}\text{He}$  are the result of the same techniques as described previously.

#### B. Mesonic Decays of ${}_{\Lambda}\text{He}$

Of the approximately 300 hyperfragments found in the emulsion pellicles scanned, about 140 mesonic decays of  ${}_{\Lambda}\text{He}$  were identified. The identification of the mesonic decays was done by an analysis of the momentum balance using the computer program for hyperfragment analysis, HANK.<sup>2</sup> From these a sample of He hyperfragments was selected whose hyperfragment prong had a range  $R_{\text{HF}} \geq 50 \mu\text{m}$  and a dip angle  $|\alpha| \leq 60^\circ$ . Since profile measurements were used in the identification of the nonmesonic  ${}_{\Lambda}\text{He}$  events, the above criteria on the range and the dip angle of the hyperfragment prong were imposed to ensure the most accurate measurements possible. Also, it was required that the hyperfragment was produced on a  $K^-$  capture star which had at least one other dark prong whose range  $\geq 5 \mu\text{m}$ . This condition was imposed for two reasons: First, it has been shown<sup>3</sup> that production of a He hyperfragment from  $K^-$  capture stars with less than one dark prong other than the hyperfragment prong is infrequent; and secondly, it minimized the  $\Sigma^-$  contamination in the nonmesonic sample since these particles are produced in a large number of cases with a pion and a very short heavy prong in the  $K^-$  capture star.

#### C. Nonmesonic Decays of ${}_{\Lambda}\text{He}$

A systematic search of all the recorded  $K^-$  stars was performed to select a sample of potential nonmesonic decays of  ${}_{\Lambda}\text{He}$ . All one- and two-pronged secondary stars (i.e., secondary stars with one or two visible decay prongs) which satisfied the abovementioned criteria on the hyperfragment or connecting track and production were included as part of the nonmesonic sample. In the case of the one pronged secondary stars, only those events with a scattering angle  $\geq 75^\circ$  and a decay prong with a range  $\geq 20 \mu\text{m}$  but  $\leq 1500 \mu\text{m}$  were considered. The scattering angle requirement and the lower limit on the decay-prong range were imposed on the one-pronged secondary stars to reduce the contamination

\* Present address: Physics Department, University of Saskatchewan, Saskatoon, Saskatchewan, Canada.

<sup>1</sup> M. W. Holland, H. G. Miller, and J. P. Roalsvig, Phys. Rev. **161**, 911 (1967).

<sup>2</sup> HANK is the Hyperfragment Analysis Kinematics program of R. G. Ammar of Northwestern University.

<sup>3</sup> D. Abeledo, L. Choy, R. G. Ammar, N. Crayton, R. Levi-Setti, M. Raymund, and O. Skjeggstad, Nuovo Cimento **15**, 181 (1960).

arising from Coulomb scattering of charge-2 particles emitted from the primary stars. The lower limit on the range of the decay prong also eliminated all contamination from the  $\pi^0$ -recoil mode of  $\Delta\text{He}^4$ , since this recoil has a characteristic range of  $\approx 9 \mu\text{m}$  and also reduced the contamination from hyperfragments with  $Z \geq 3$ . The upper limit of  $1500 \mu\text{m}$  was selected since this represents a range slightly greater than the maximum range of a single recoil from a nonmesonic decay of  $\Delta\text{He}^4$  or  $\Delta\text{He}^5$  allowed by kinematics.

An image-splitting eyepiece was used to make the profile or track thickness measurements. Thickness measurements were made on the connecting or hyperfragment track at intervals of 1 or  $2 \mu\text{m}$ , depending on the track length and starting at a distance of  $20 \mu\text{m}$  from the secondary (or decay) vertex. Up to  $30 \mu\text{m}$  of track were profiled in this manner, and the depth in the emulsion of the center of the profiled segment of track was recorded. The last  $20 \mu\text{m}$  of a track was not profiled because of the characteristic narrowing of tracks as they come to rest in the emulsion.

The charge-2 standards were selected from the previously identified mesonic decays of  $\Delta\text{He}$ .  $\Sigma^+$  particles

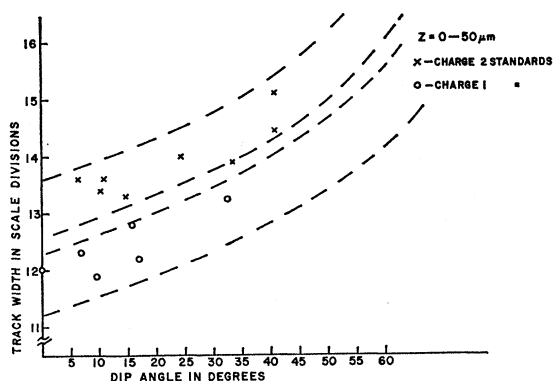


FIG. 1. Profile measurements of charge-1 and charge-2 standards at depth  $Z=0-50 \mu\text{m}$ .

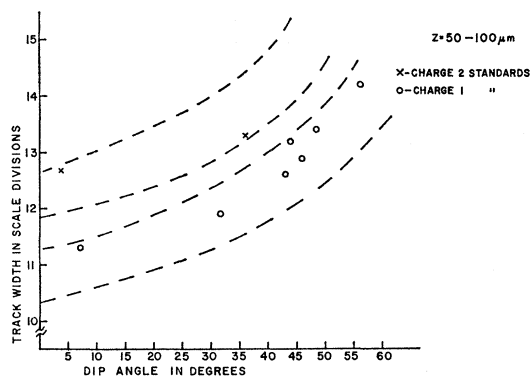


FIG. 2. Profile measurements of charge-1 and charge-2 standards at depth  $Z=50-100 \mu\text{m}$ .

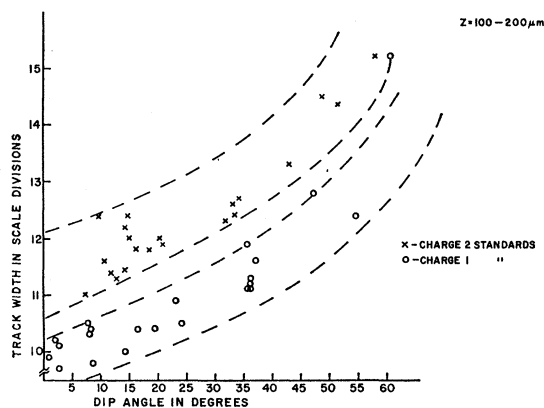


FIG. 3. Profile measurements of charge-1 and charge-2 standards at depth  $Z=100-200 \mu\text{m}$ .

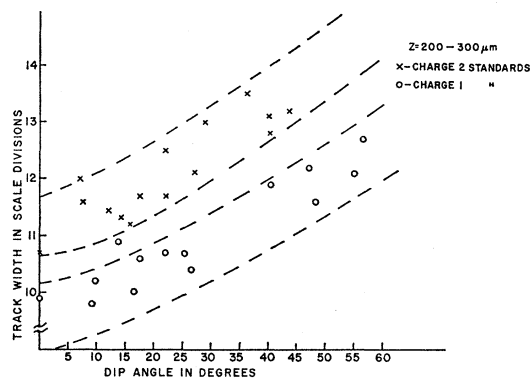


FIG. 4. Profile measurements of charge-1 and charge-2 standards at depth  $Z=200-300 \mu\text{m}$ .

which decay at rest into a  $\pi^0$  and a visible proton of characteristic range were used as charge-1 standards. Forty-five charge-2 standards and 47 charge-1 standards were profiled. Since a variation in development with depth in the emulsion pellicles was observed, the graphs of average track width versus dip angle were plotted at different depth intervals (Figs. 1-4). The charge-1 and -2 regions were determined for each depth interval and are represented on the graphs by the dashed lines, the charge-1 region being the lower in each case. At all depths, there was a distinct separation of the charge-2 region from the charge-1 region. These regions were then used to determine the charge of the unknown connecting tracks for the events in the nonmesonic sample.

All the recorded decays with two visible decay prongs were analyzed kinematically using the program HANK in an attempt to determine the nonmesonic decay modes. In each case it was assumed that only one neutron was emitted. The visible decay prongs were assumed, in turn, to be either a proton, a deuteron, or a triton, and the binding energy  $B_\Delta$  was calculated for each permutation.

### III. RESULTS

#### A. Mesonic decays of $\Lambda\text{He}$

Forty-seven mesonic decays of  $\Lambda\text{He}$ , which fit the aforementioned criteria, were identified. Table I lists the events observed. A histogram of the recoil ranges of all the  $\Lambda\text{He} \rightarrow \pi^- p r$  decays is given in Fig. 5. The cross-hatched area of the histogram represents the 47 events in the mesonic sample. In the case of the ambiguous  $\Lambda\text{He}$  events with very short recoil prongs, the calculated recoil momentum was used to determine the range of the recoils. (For very short ranges the  $\text{He}^3$  momentum is approximately equal to the  $\text{He}^4$  momentum.)

In order to calculate the nonmesonic-to-mesonic ratio for  $\Lambda\text{He}^5$ , it is necessary to determine the number of mesonic decays of  $\Lambda\text{He}^4$  and  $\Lambda\text{He}^5$  in the mesonic sample. Since the number of events identified in the sample is small, it was decided to use the data given by Ammar *et al.*<sup>4</sup> to estimate the number of  $\Lambda\text{He}^4$  and  $\Lambda\text{He}^5$  events in our mesonic sample. Out of 53 identified mesonic decays of  $\Lambda\text{He}^{4,5}$  (whose hyperfragment prong was  $> 50 \mu\text{m}$ ) observed by Ammar *et al.*,<sup>4</sup> 15 were found to be mesonic decays of  $\Lambda\text{He}^4$ . This yields a decay ratio,  $R(\Lambda\text{He}^4/\Lambda\text{He}^5) \simeq 0.39$ . Using this ratio, it is estimated that 13 of the 47 events in our mesonic sample are  $\Lambda\text{He}^4$  and 34 are  $\Lambda\text{He}^5$ . (The  $\Lambda\text{He}^7$  contamination, which is small, is ignored.)

A histogram of the hyperfragment ranges of the 47 events in the mesonic sample is given in Fig. 6. A similar plot (Fig. 7) for the nonmesonic sample is given for comparison. The distributions are in close agreement.

#### B. Nonmesonic Decays of $\Lambda\text{He}$

The results of the profile measurements on the connecting tracks of the approximately 150 events in the nonmesonic sample are given in Figs. 8–11. The charge-1 and -2 regions, which have been determined from profile measurements made on the standards (see Figs. 1–4), are indicated by the dashed lines, the charge-1 region being the lower for each depth interval. Forty-six two-pronged and five one-pronged events were found to have charge-2 connecting tracks. In four of the five one-pronged events, the decay prong was greater than  $35 \mu\text{m}$  and therefore it was possible to identify it, by a profile measurement, as a charge-2 track also.

All 46 two-pronged events were analyzed kinematically using HANK to determine whether or not they could be fitted as nonmesonic decays of He hyperfragments with only one neutron emitted in the decay. An event was considered to be kinematically fitted if the binding energy  $B_\Lambda$  of the decay mode was within  $\pm 8 \text{ MeV}$  of the binding energy of its mesonic counterpart, where the binding energies of the mesonic decays of  $\Lambda\text{He}^4$  and  $\Lambda\text{He}^5$  have been taken to be  $2.27 \pm 0.10 \text{ MeV}$  and  $3.21 \pm 0.03 \text{ MeV}$ ,<sup>5,6</sup> respectively. A list of the fitted events with the energy of the decay particles is given in Table II. A histogram of the binding energies  $B_\Lambda$  of all the uniquely fitted events which meet the abovementioned binding energy criteria is given in Fig. 12.

Histograms of the momentum of the decay particles from the proton-stimulated decays of  $\Lambda\text{He}^4$  and the proton-stimulated decays of  $\Lambda\text{He}^5$  are given in Figs. 13 and 14. Figure 14 also contains a histogram of the

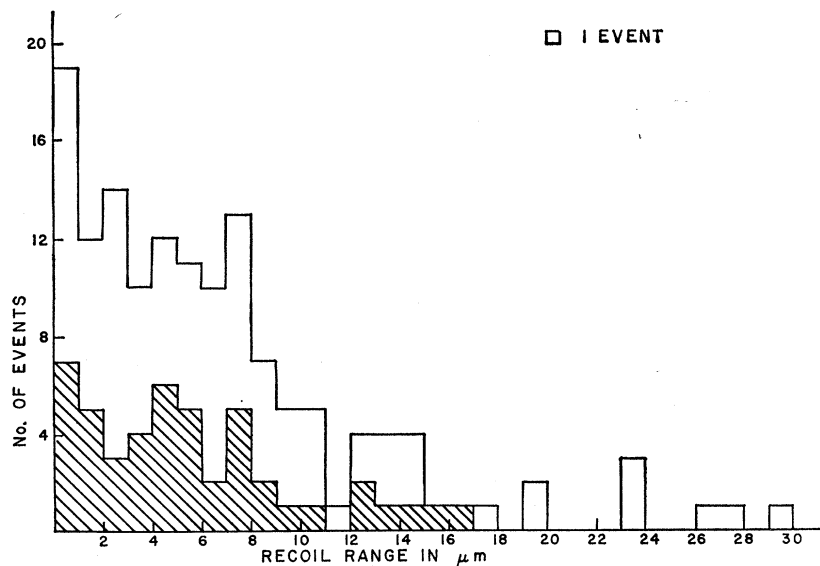


FIG. 5. The recoil ranges of all the mesonic  $\Lambda\text{He}$  decays. The cross-hatched area represents the 47 events in the mesonic sample.

<sup>4</sup> R. G. Ammar, R. Levi-Setti, W. E. Slater, S. Limentani, P. E. Schlein, and P. H. Steinberg, *Nuovo Cimento* **19**, 20 (1961).

<sup>5</sup> C. Mayeur *et al.*, *Nuovo Cimento* **43A**, 180 (1966).

<sup>6</sup> A. H. Rosenfeld, A. Barbaro-Gatheri, W. J. Podolsky, L. R. Price, P. Soding, C. G. Wohl, M. Roos, and W. J. Willis, *Rev. Mod. Phys.* **39**, 1 (1967). We use their values to obtain the  $Q$  for free  $\Lambda$  decay as  $37.74 \text{ MeV}$  as compared to  $Q=37.58 \text{ MeV}$  in Ref. 5.

TABLE I. Events in the mesonic sample.

Hypernucleus	Number	Decay mode
$\Delta\text{He}^4$	5	$\pi p r$
$\Delta\text{He}^5$	19	$\pi p r$
$\Delta\text{He}^7$	1	$\pi p r$
ambiguous $\Delta\text{He}$	22	$\pi p r$

momentum of the decay prong from one-pronged events, where the decay prong is assumed to be  $\Delta\text{He}^3$  from decay  $\Delta\text{He}^5 \rightarrow n+n+\text{He}^3$ . The momentum distributions of both  $\text{H}^3$  and  $\text{He}^3$  are in close agreement.

### C. Correction Factors

#### 1. Detection Efficiency

A random sample of approximately 1000  $K^-$  capture stars (or approximately 3% of the total number of  $K^-$  stars) was reexamined by a second observer for one and two-pronged nonmesonic  $\Delta\text{He}$  events. In both scanings the number of events detected was the same, which implies a 100% detection efficiency for this

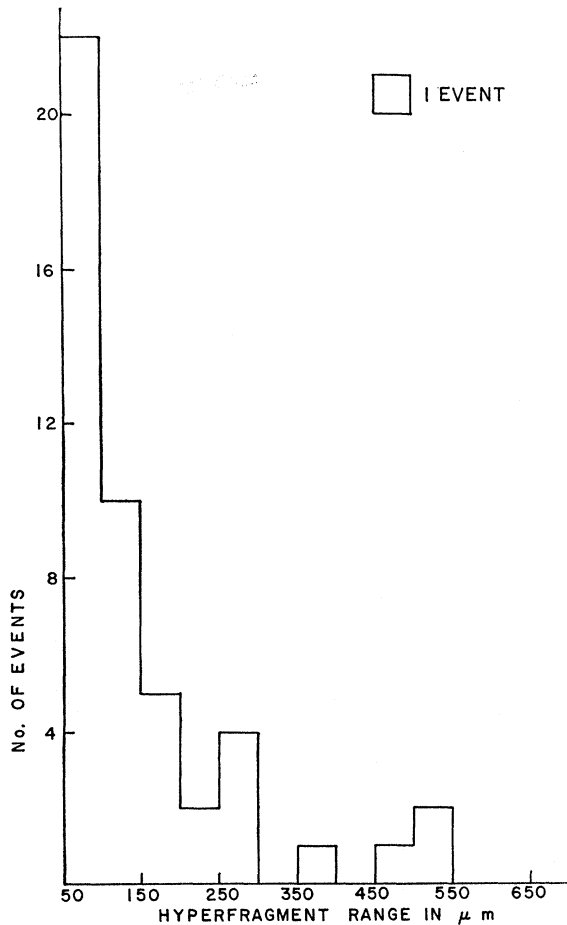


FIG. 6. Hyperfragment ranges of the 47 events in the mesonic  $\Delta\text{He}$  sample.

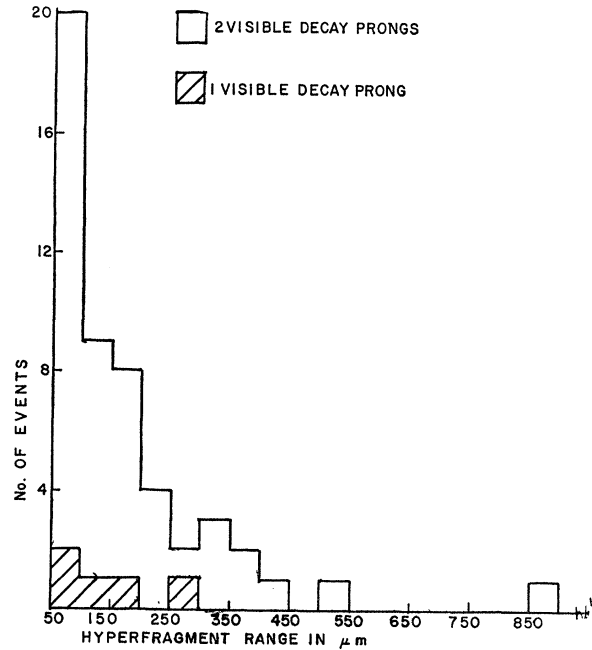


FIG. 7. Hyperfragment ranges of the 51 events in the nonmesonic  $\Delta\text{He}$  sample.

subset of 1000 stars. On this basis, it seems probable that the detection efficiency for the whole sample of  $K^-$  capture stars is certainly greater than 85%. Because of this, no correction for detection efficiency was deemed necessary.

TABLE II. Data of fitted events of nonmesonic decays of  $\Delta\text{He}^{4,5,a}$

Event	Fit	Prong energy (MeV)		$B_\Delta$ (MeV)	
26-62	$d+d+n$	2.34 ( <i>d</i> )	47.89 ( <i>d</i> )	105.56 ( <i>n</i> )	3.73
28-52	$p+t+n$	56.90 ( <i>p</i> )	5.37 ( <i>t</i> )	91.98 ( <i>n</i> )	1.85
28-54	$p+t+n$	6.60 ( <i>p</i> )	10.13 ( <i>t</i> )	98.77 ( <i>n</i> )	6.90
28-56	$t+t+n$	91.08 ( <i>t</i> )	38.52 ( <i>t</i> )	34.46 ( <i>n</i> )	-0.42
29-55	$d+d+n$	34.84 ( <i>d</i> )	9.31 ( <i>d</i> )	111.61 ( <i>n</i> )	-3.68
30-51	$p+t+n$	66.54 ( <i>p</i> )	3.31 ( <i>t</i> )	77.30 ( <i>n</i> )	8.96
33-64	$p+t+n$	31.54 ( <i>p</i> )	50.55 ( <i>t</i> )	110.47 ( <i>n</i> )	-0.51
	$p+d+n$	9.38 ( <i>p</i> )	42.55 ( <i>d</i> )	119.05 ( <i>d</i> )	-0.56
36-52	$p+d+n$	94.03 ( <i>p</i> )	33.85 ( <i>d</i> )	47.36 ( <i>n</i> )	-4.82
36-56	$d+d+n$	38.67 ( <i>d</i> )	2.59 ( <i>d</i> )	107.15 ( <i>n</i> )	3.67
36-60	$p+t+n$	91.14 ( <i>p</i> )	1.56 ( <i>t</i> )	56.63 ( <i>n</i> )	6.77
42-53	$p+d+n$	34.84 ( <i>p</i> )	15.26 ( <i>d</i> )	116.71 ( <i>n</i> )	3.62
43-65	$p+d+n$	90.66 ( <i>p</i> )	0.48 ( <i>d</i> )	78.94 ( <i>n</i> )	0.35
47-51	$p+t+n$	67.43 ( <i>p</i> )	4.94 ( <i>t</i> )	85.20 ( <i>n</i> )	-1.47
49-61	$p+t+n$	57.47 ( <i>p</i> )	18.09 ( <i>t</i> )	85.60 ( <i>n</i> )	-5.00
50-56	$p+t+n$	7.31 ( <i>p</i> )	38.43 ( <i>t</i> )	111.01 ( <i>n</i> )	-0.64
50-60	$p+t+n$	104.93 ( <i>p</i> )	24.83 ( <i>t</i> )	19.63 ( <i>n</i> )	6.72
53-59	$t+t+n$	16.29 ( <i>t</i> )	12.54 ( <i>t</i> )	130.23 ( <i>n</i> )	4.59
53-61	$p+t+n$	110.41 ( <i>p</i> )	21.83 ( <i>t</i> )	18.93 ( <i>n</i> )	4.94
64-52	$p+t+n$	24.00 ( <i>p</i> )	15.58 ( <i>t</i> )	108.99 ( <i>n</i> )	7.54
67-52	$p+d+n$	48.60 ( <i>p</i> )	8.32 ( <i>d</i> )	110.54 ( <i>n</i> )	2.96
70-52	$d+d+n$	51.83 ( <i>d</i> )	14.82 ( <i>d</i> )	85.94 ( <i>n</i> )	-0.52

<sup>a</sup> Complete data for all nonmesonic events are given in H. G. Miller, M.A. thesis, State University of New York at Buffalo, 1967 (unpublished).

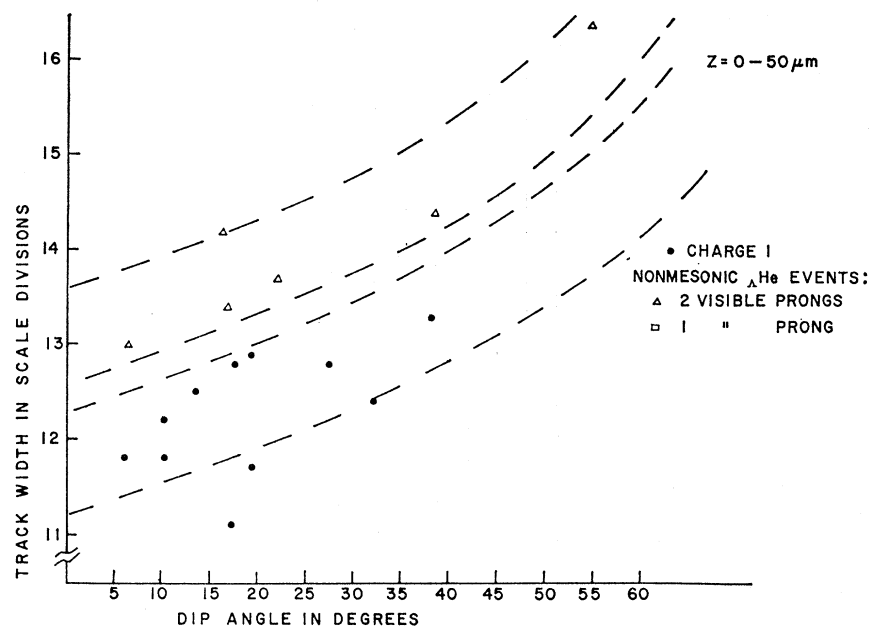


FIG. 8. Profile measurements of nonmesonic sample at depth  $Z=0-50 \mu\text{m}$ .

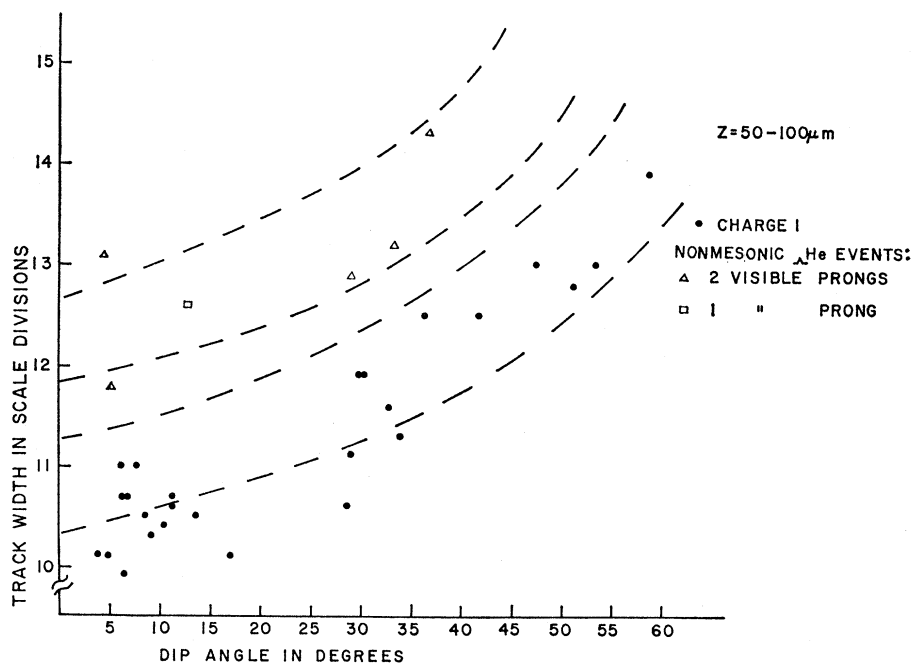


FIG. 9. Profile measurements of nonmesonic sample at depth  $Z=50-100 \mu\text{m}$ .

## 2. $\pi^0$ Contamination

Not all of the 51 events found to have charge-2 connecting tracks are examples of nonmesonic decays of He hyperfragments. There is another competing decay mode of He hyperfragments, the  $\pi^0$  decay mode, which must be accounted for. Table III lists the possible  $\pi^0$  decay modes of  $\Delta^4\text{He}^{4,5}$ .

Decay modes 1-4 occur with one visible decay prong and, therefore, contamination arising from these modes will appear only in 5 of the observed 51 events in the

nonmesonic sample. Since mode 3 is a two-body decay, the recoil ( $\text{He}^4$ ) range is unique and is known to be about  $9 \mu\text{m}$ . Hence, no contamination from this mode is possible since only one-pronged events with a decay prong  $\geq 20 \mu\text{m}$  were included in the nonmesonic sample. The contamination arising from modes 1 and 4 can be estimated by looking at the recoil ranges of the mesonic ( $\pi^-p \text{He}^{3,4}$ ) decays (Fig. 5). Of the total of 142  $\pi^-p$  modes observed, only six events (or 4.2%) had a range greater than  $20 \mu\text{m}$ . None of these six events, however, were part of the 47 events in the mesonic sample.

FIG. 10. Profile measurements of nonmesonic sample at depth  $Z=100-200 \mu\text{m}$ .

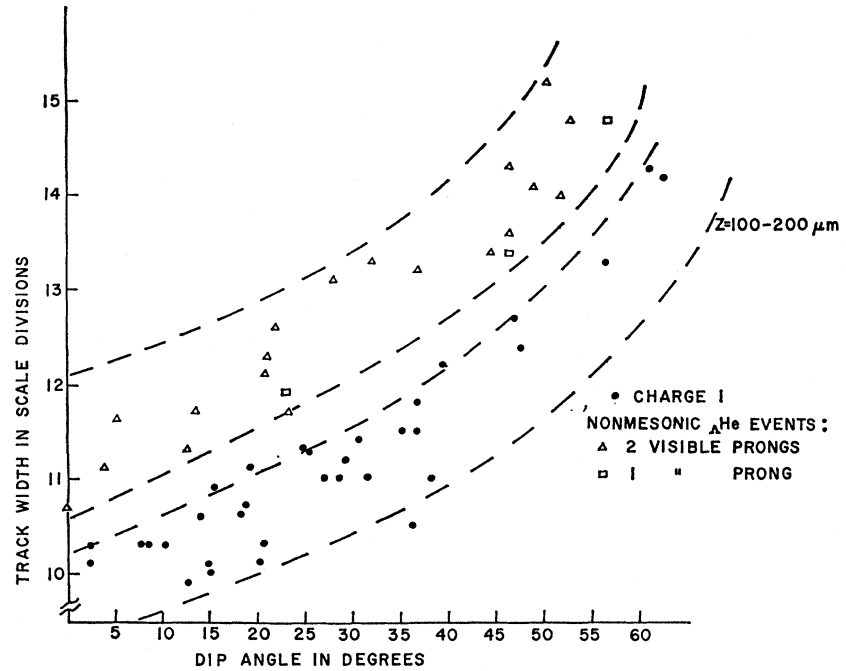
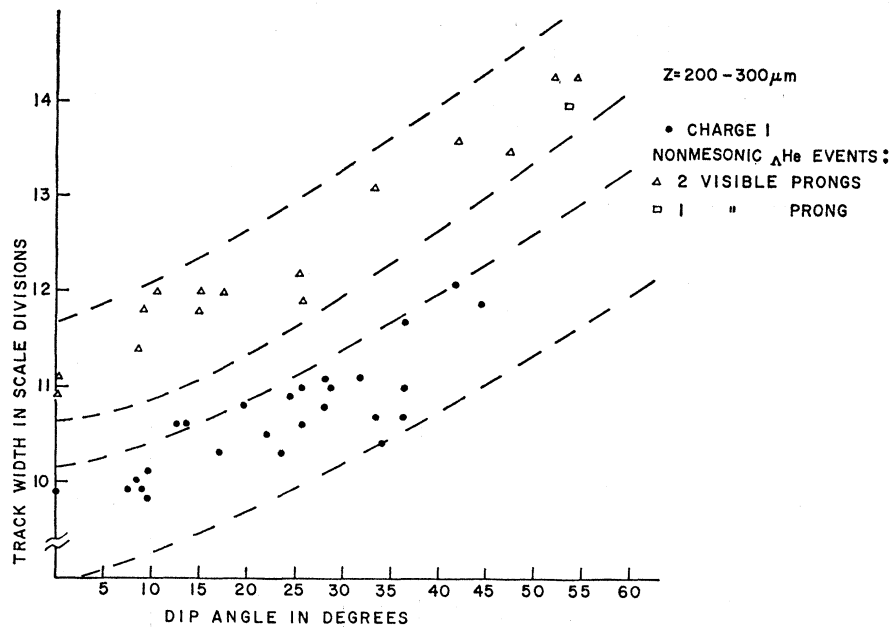


FIG. 11. Profile measurements of nonmesonic sample at depth  $Z=200-300 \mu\text{m}$ .



Furthermore, the dominance of the  $\pi^0 \text{He}^4$  decay mode for  $\Delta\text{He}^4$  minimizes the number of decays of  $\Delta\text{He}^4$  by mode 4. Assuming the recoil range distribution to be somewhat similar to that for the  $\pi^- \text{pr}$  modes, contamination from the modes 1 and 4 is estimated to be much less than one event and can thus be considered negligible. No contamination is expected from mode 2 since the great stability of the  $\text{He}^4$  core nucleus results in a domination of the  $\pi^0 n \text{He}^4$  mode in the  $\pi^0$  decays of  $\Delta\text{He}^5$  hyperfragments.

An estimate of the contamination arising from the remaining  $\pi^0$  decays of  $\Delta\text{He}$ , with two visible decay prongs, can be made by looking at the branching ratios of the charge symmetric states for the mesonic decay modes of  $\Delta\text{H}^4$ . Table IV lists the identified mesonic decay modes (and the number of each mode observed) of  $\Delta\text{H}^4$ , with a hyperfragment prong  $\geq 50 \mu\text{m}$ , observed by Ammar *et al.*<sup>4</sup> Now, assuming the  $\pi^-$  decay modes of  $\Delta\text{H}^4$  are the charge symmetric states of the  $\pi^0$  decay modes of  $\Delta\text{He}^4$ , the branching ratio of the number of

decays of modes 3-6 (Table IV) of  $\Delta\text{H}^4$  to the total number of  $\pi^-$  decays of  $\Delta\text{H}^4$  should be comparable to the branching ratio of the number of decay modes 5-8

(Table III) of  $\Delta\text{He}^4$ . Seven out of 69  $\pi^-$  decays of  $\Delta\text{H}^4$  are examples of modes 3-6 (Table IV), yielding a branching ratio

$$R_{\pi^0} = \frac{\text{number of decays of } \Delta\text{He}^4 \text{ through modes 5-8 in Table III}}{\text{all } \pi^0 \text{ modes of } \Delta\text{He}^4} = \frac{7}{69} \approx 0.10.$$

This implies that about 10% of the  $\pi^0$  decays of  $\Delta\text{He}^4$  are modes with two visible prongs (modes 5-8 in Table III). Using results given by Ammar *et al.*<sup>4</sup> for the mesonic decay ratio of  $\Delta\text{He}^5$  to  $\Delta\text{He}^4 + \Delta\text{He}^5$ ,  $R_{\text{mesonic}} = \Delta\text{He}^4 / (\Delta\text{He}^4 + \Delta\text{He}^5) \approx 0.28$ , and the value obtained

by Block *et al.*<sup>7</sup> for the decay ratio of  $\pi^0$  to  $\pi^-$  decays of  $\Delta\text{He}^4$ ,  $R_{\Delta\text{He}^4}(\pi^0/\pi^-) \approx 2.5$ , the  $\pi^0$  contamination ( $C_{\pi^0}$ ) from the modes 5-8 in the nonmesonic sample is estimated using the following:

$$C_{\pi^0} \approx N_{\text{mesonic}} R_{\Delta\text{He}^4}(\pi^0/\pi^-) R_{\text{mesonic}} R_{\pi^0}$$

$\approx 3.2$  events, or approximately 3 events, where  $N_{\text{mesonic}}$  is the number of decays of  $\Delta\text{He}^4 + \Delta\text{He}^5$  in the mesonic sample.

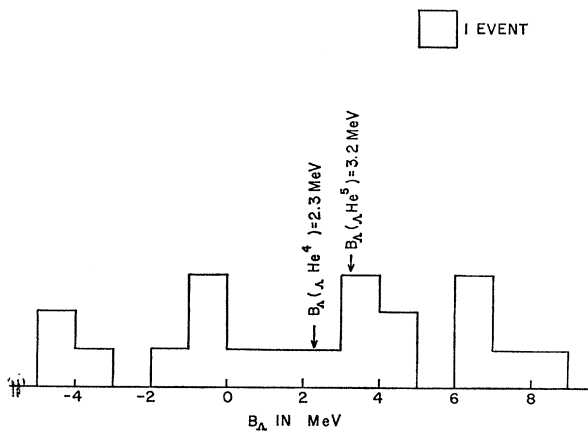


FIG. 12. Binding energies of all the uniquely fitted nonmesonic decays of  $\Delta\text{He}^{4,5}$ .

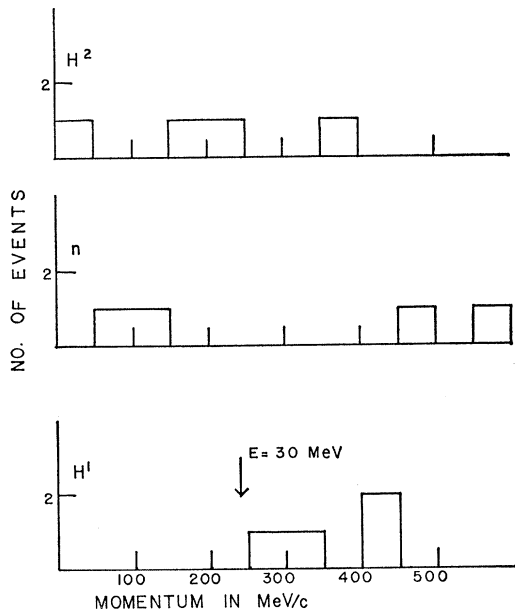


FIG. 13. Momentum of decay particles from  $\Delta\text{He}^4 \rightarrow \text{H}^1 + \text{H}^2 + n$ .

### 3. Coulomb Scattering

Another source of contamination which must be considered in the case of the one-pronged events, arises from Coulomb scattering of charge-2 particles emitted from the primary star. In order to estimate the amount of contamination due to Coulomb scattering, all of the dark prongs, with ranges  $\geq 70 \mu\text{m}$  and a dip angle

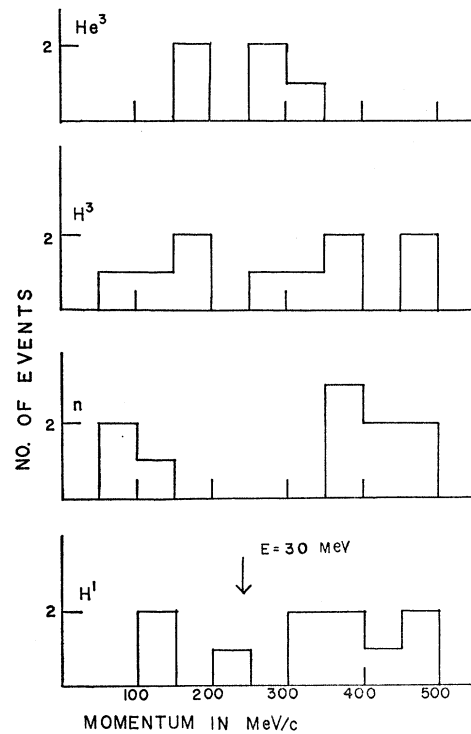


FIG. 14. Momentum of decay particles from  $\Delta\text{He}^5 \rightarrow \text{H}^1 + \text{H}^3 + n$  and momentum of the visible decay prong of the one-pronged events, assuming it to be  $\text{He}^3$  from  $\Delta\text{He}^5 \rightarrow n + n + \text{He}^3$ .

<sup>7</sup> M. M. Block, *et al.*, in *Proceedings of the International Conference on Hyperfragments* (CERN, Geneva, 1964), p. 63.

$|\alpha| \leq 60^\circ$  from 60 (out of 35 000  $K^-$  capture stars in the sample) randomly selected  $K^-$  capture stars which emitted no  $\Sigma$  particles or hyperfragments, were profiled to determine the number of charge-2 prongs present. The ranges of these charge-2 tracks were measured and the residual range of the tracks determined. The residual range is the range of a track measured from the end of the track to a point  $50 \mu\text{m}$  (which is the minimum length of a connecting track in the mesonic and non-mesonic sample) from the  $K^-$  capture star where the track was produced. The residual range represents the amount of track in which a scattering would have been observed had it occurred. The number of charge-2 tracks from the sample of 60 stars whose residual range lies in various range intervals (Table V) was determined. Correcting for the number of charge-2 tracks in each interval expected in the total sample of  $K^-$  capture stars, and using a curve of the probability of scattering per micrometer for  $\alpha$  particles versus residual range for scattering angles greater than  $75^\circ$  given by Kenyon *et al.*,<sup>8</sup> the number of events in each range interval arising from Coulomb scattering can be calculated. These results are given in Table V. The total number of events expected between  $20 \mu\text{m}$  (the minimum range of one-prong events) and  $400 \mu\text{m}$  is approximately three events. Since all five of the one-prong events observed had recoil ranges between  $20$  and  $400 \mu\text{m}$ , it is estimated, therefore, that about three one-pronged events are the result of Coulomb scattering. However, three of the five one-pronged events display all the characteristics of decay stars and are considered to be nonmesonic decays of  $\Delta\text{He}$ . Therefore, it is estimated that only the remaining two events are the contamination arising from Coulomb scattering.

#### 4. Contamination for $Z \geq 3$ Events

Out of the total number of hyperfragments observed in the plates scanned, two  $\pi^-$  decays of heavier hyperfragments ( $Z \geq 3$ ) were found which satisfied the criteria specified for the selection of events in the mesonic  $\Delta\text{He}$  sample. Both were ambiguous decays of  $\Delta\text{Li}$ . This implies that there would be about five nonmesonic  $\Delta\text{Li}$

TABLE III.  $\pi^0$  decay modes of  $\Delta\text{He}^{4,5}$ .

(1)	$\Delta\text{He}^5 \rightarrow \pi^0 + n + \text{He}^4$
(2)	$\rightarrow \pi^0 + n + n + \text{He}^3$
(3)	$\Delta\text{He}^4 \rightarrow \pi^0 + \text{He}^4$
(4)	$\rightarrow \pi^0 + n + \text{He}^3$
(5)	$\rightarrow \pi^0 + n + p + d$
(6)	$\rightarrow \pi^0 + p + t$
(7)	$\rightarrow \pi^0 + d + d$
(8)	$\rightarrow \pi^0 + p + p + n + n$

TABLE IV.  $\pi^-$  decays of  $\Delta\text{H}^4$  observed by Ammar *et al.*<sup>9</sup>

	No. of events observed
(1) $\Delta\text{H}^4 \rightarrow \pi^- + \text{He}^4$	46
(2) $\rightarrow \pi^- + p + \text{H}^3$	16
(3) $\rightarrow \pi^- + p + n + \text{H}^2$	1
(4) $\rightarrow \pi^- + n + \text{He}^3$	4
(5) $\rightarrow \pi^- + d + d$	2
(6) $\rightarrow \pi^- + p + p + n + n$	0

\* Reference 4.

events,<sup>9</sup> some of which may decay with the emission of two visible decay prongs, therefore fitting the aforementioned criteria of selection of events. However, no  $Z \geq 3$  events were detected in profile measurements made on events selected as possible nonmesonic  $\Delta\text{He}$  candidates. Therefore, no correction was made for contamination from  $Z \geq 3$  events.

#### D. Ratio of Nonmesonic to $\pi^-$ Decays in $\Delta\text{He}$

Correcting the nonmesonic sample for  $\pi^0$  and Coulomb scattering contamination and for the scattering volume eliminated by the scattering criteria imposed (the angles accepted included only 63% of the scattering volume), the number of nonmesonic events ( $N_{\text{nonmesonic}}$ ) in the sample is 48. Since there were 47  $\pi^-$  decays in the mesonic sample, the nonmesonic to mesonic ratio  $[Q(\Delta\text{He})]$  for  $\Delta\text{He}$  is given by

$$Q(\Delta\text{He}) = 48/47 = 1.02 \pm 0.15.$$

TABLE V. Data for determining the number of  $Z=2$  particles arising from Coulomb scattering.

Residual range ( $\mu\text{m}$ )	Number of $Z=2$ prongs in sample of 60 randomly selected $K^-$ capture stars	Number of $Z=2$ prongs expected in total sample of 35 000 $K^-$ stars	Probability of scattering per $\mu\text{m}$ for $\alpha$ particles, with scattering angle $\geq 75^\circ$	Number of events which arise from Coulomb scattering of $Z=2$ particles
20-30	12	7000	$12 \times 10^{-6}$	0.8
30-40	10.6	6200	8	0.5
40-60	10	5800	5	0.6
60-100	9	5200	2	0.4
100-200	7.4	4300	1	0.4
200-300	6.1	3500	$\sim 0.5$	0.2
300-400	13.2	7700	$< 0.1$	$< 0.1$

<sup>8</sup> I. R. Kenyon, A. Z. Ismail, A. W. Key, S. Lokanathan, and Y. Prakash, *Nuovo Cimento* **30**, 1365 (1963).

<sup>9</sup> M. W. Holland, *Nuovo Cimento* **32**, 33 (1964).

Also, it is now possible to determine the nonmesonic-to-mesonic ratio  $Q(\Lambda\text{He}^5)$  for  $\Lambda\text{He}^5$ . Previously the number of  $\Lambda\text{He}^4$  and  $\Lambda\text{He}^5$  events in the mesonic sample was estimated to be 13 and 34, respectively. Using the value of Block *et al.*<sup>7</sup> for nonmesonic-to-mesonic ratio of  $\Lambda\text{He}^4$ ,  $Q(\Lambda\text{He}^4)=0.52\pm 0.10$ , the number of nonmesonic decays of  $\Lambda\text{He}^4$  in the sample is then estimated to be of the order of seven events. Therefore, it is estimated that 41 of the 48 events in the nonmesonic sample are decays of  $\Lambda\text{He}^5$  (again neglecting  $\Lambda\text{He}^7$  events). This implies a nonmesonic-to-mesonic ratio for  $\Lambda\text{He}^5$  hyperfragments:

$$Q(\Lambda\text{He}^5)=1.21\pm 0.19.$$

### E. Ratio of Proton to Neutron Stimulation

Certain problems arise in determining the ratio of proton stimulation to neutron stimulation, denoted by  $C=\Delta p/\Delta n$  (where  $\Delta p$ =number of proton stimulation events and  $\Delta n$ =number of neutron stimulation events), since there is no clearly defined method by which either the proton or neutron stimulated events may be identified. In Fig. 15, a histogram is given for the kinetic energy of the "protons" for the 46 two-body nonmesonic events, where the longest prong of the decay in each case has been assumed to be a proton. No clearly defined cutoff value distinguishes "fast protons" from proton stimulated events. However, as has been done previously,<sup>10</sup> a cutoff value of 20–35 MeV has been assumed for the selection of proton stimulated events. Using proton energies of 20, 25, 30, and 35 MeV as the cutoff values, the number of protons with energies above the different cutoff values has been determined and the respective values of  $C(\Lambda\text{He})$  for all the non-

mesonic decays of  $\Lambda\text{He}$  have been calculated. The values of  $C(\Lambda\text{He})$  are given in Table VI.

Once  $C(\Lambda\text{He})$  has been determined the ratio of the number of proton to neutron stimulated events for  $\Lambda\text{He}^5$ ,  $C(\Lambda\text{He}^5)=(\Delta p)_5/(\Delta n)_5$ , can be calculated in the following manner. The ratio of proton to neutron stimulation for  $\Lambda\text{He}$  is defined as

$$C(\Lambda\text{He})=\frac{(\Delta p)_4+(\Delta p)_5}{(\Delta n)_4+(\Delta n)_5} \\ =\frac{C_4[1/(\Delta n)_5]+C_5[1/(\Delta n)_4]}{[1/(\Delta n)_5]+[1/(\Delta n)_4]}, \quad (1)$$

where

$$C_5=(\Delta p)_5/(\Delta n)_5, \\ C_4=(\Delta p)_4/(\Delta n)_4=2.2\pm 0.8.^7$$

The number of nonmesonic decays of  $\Lambda\text{He}^4$  and  $\Lambda\text{He}^5$  hyperfragments has already been estimated to be 7 for  $\Lambda\text{He}^4$  and 41 for  $\Lambda\text{He}^5$ .

TABLE VI. Values of  $C$  and  $C_5$  for different cutoff energies ( $E_{\text{max}}^p$ ) of the fast protons.

Cutoff energy ( $E_{\text{max}}^p$ ) of fast protons in MeV	No. of events with fast protons (proton stimulated events)	No. of neutron stimulated events (=48–No. of proton stimulated events)	$C$	$C_5$
20	28	20	1.4	1.3
25	24	24	1.0	0.9
30	20	28	0.7	0.6
35	18	30	0.6	0.5

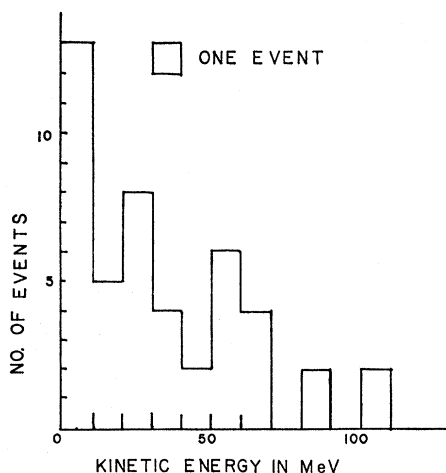


FIG. 15. Kinetic energy of the longest prong observed in the 46 two-pronged nonmesonic  $\Lambda\text{He}$  events, where this prong has been assumed to be a proton.

<sup>10</sup> M. Baldo-Ceolin, C. Dilworth, W. F. Fry, W. D. B. Greening, H. Huzita, S. Limentani, and A. E. Sichirollo, *Nuovo Cimento* 7, 328 (1958).

The following results are thus obtained:

$$(\Delta n)_4=7/(C_4+1)=2.2, \\ (\Delta n)_5=41/(C_5+1),$$

which, when substituted along with the value of  $C_4$  into Eq. (1), yields

$$C_5=(43.2C-4.8)/(45.8-2.2C). \quad (2)$$

The values of  $C_5$  for different values of  $C$  are also listed in Table VI.

## IV. DISCUSSION OF RESULTS

### A. Comparison with Previous Experimental Results

Table VII lists the values for  $Q(\Lambda\text{He})$  and  $C$  from previous works. The present value of  $Q(\Lambda\text{He})$  is somewhat lower than previous measurements. However, within the experimental errors, it is still in agreement with all of the previous results.

In the case of  $C$ , only two other values have been determined previously for  $\Lambda\text{He}$  separately. The value

TABLE VII. Values of  $Q(\Delta\text{He})$  and  $C$  obtained in previous works.

Authors	$Q(\Delta\text{He})$	$C(\Delta Z^{A+1})$
Schneps, Fry, Swami <sup>a</sup> Silverstein <sup>b</sup>	$\leq 2.6$ $0.6 < Q < 1.4$ for $R_{Hf} > 20 \mu\text{m}$	1.1 for $E_{\text{max}}^p = 30 \text{ MeV}$ and $R_{Hf} \geq 20 \mu\text{m}$ 0.6 for $E_{\text{max}}^p = 40 \text{ MeV}$ and $Z \geq 2$
Baldo-Ceolin <i>et al.</i> <sup>c</sup>		0.7 for $R_{Hf} \geq 20 \mu\text{m}$ 2 or more prongs $Z = 2, 3, 4$ $E_{\text{max}}^p = 30 \text{ MeV}$
Berkovich <i>et al.</i> <sup>d</sup>		0.8 for $R_{Hf} \geq 20 \mu\text{m}$ $E_{\text{max}}^p = 26 \text{ MeV}$ $Z \geq 2$
J. Sacton <sup>e</sup>	$\sim 1.2$	1.3 for $E_{\text{max}}^p = 25 \text{ MeV}$ and $Z \geq 2$ 1.2 for $E_{\text{max}}^p = 30 \text{ MeV}$ and $Z \geq 2$
Gorge <i>et al.</i> <sup>f</sup>	$\sim 1.2$	0.8 for $E_{\text{max}}^p = 20 \text{ MeV}$ and $Z = 2, 3$ 0.4 for $E_{\text{max}}^p = 30 \text{ MeV}$
P. E. Schlein <sup>g</sup> Bhowmik <i>et al.</i> <sup>h</sup>	$\geq 1.5 \pm 0.4$ for $R_{Hf} \geq 59 \mu\text{m}$ , 2 prong events only $\sim 1.4$	$\sim 2.5$ for $Z \geq 3$ $\sim 3.8$ for $Z = 2$ and $E_{\text{max}}^p = 25 \text{ MeV}$
Kenyon <i>et al.</i> <sup>i</sup>	$1.3 \leq Q \leq 3.0$ (same selection as used in present work, except $R_{Hf} \geq 40 \mu\text{m}$ )	$\geq 0.7$ for $\Delta\text{He}^5$
Our result	$Q(\Delta\text{He}) = 1.0 \pm 0.2$ $Q(\Delta\text{He}^5) = 1.2 \pm 0.2$	See Table VI

<sup>a</sup> J. Schneps, W. F. Fry, and M. S. Swami, Phys. Rev. **106**, 1062 (1957).<sup>b</sup> E. M. Silverstein, Nuovo Cimento Suppl. **10**, 41 (1958).<sup>c</sup> Reference 10.<sup>d</sup> I. B. Berkovich, A. P. Zhadanov, F. G. Lepekhin, and Z. S. Knokhlova, Zh. Eksp. i Teor. Fiz. **38**, 423 (1960) [English transl.: Soviet Phys.—JETP **11**, 311 (1960)].<sup>e</sup> J. Sacton, Nuovo Cimento **18**, 266 (1960).<sup>f</sup> V. Gorge, W. Koch, W. Lindt, M. Nikolic, S. Subotic-Nikolic, and H. Winzeler, Nucl. Phys. **21**, 599 (1960).<sup>g</sup> P. E. Schlein, Phys. Rev. Letters **2**, 220 (1959).<sup>h</sup> References 11 and 12.<sup>i</sup> Reference 8.

$C(\Delta\text{He}) = 3.8$  obtained by Bhowmik *et al.*<sup>11,12</sup> is obtained employing no range requirement on the hyperfragment prongs. The value  $C_5 \geq 0.7$ , obtained by Kenyon *et al.*,<sup>8</sup> is in agreement with the present results, taking a cutoff energy  $E_{\text{max}}^p \leq 25 \text{ MeV}$ .

### B. Theoretical Considerations

A theoretical method for calculating the non-mesonic decay rates has been given by Dalitz *et al.*<sup>13-17</sup> This method treats the  $\Lambda$  de-excitation by different nucleons as incoherent. Also, it neglects final-state interactions for two fast outgoing nucleons, and the interference effects which usually arise from antisymmetrization of the final state, corrections which are not expected to be important here, because of the large energy release. A similar treatment for He hyperfragments is presented in the following.

$R_{NS}$  is defined as the  $\Lambda N \rightarrow NN$  transition rate for

<sup>11</sup> B. Bhowmik, D. P. Goyal, and N. K. Yamdagni, Phys. Letters **3**, 13 (1962).<sup>12</sup> B. Bhowmik, D. P. Goyal, and N. K. Yamdagni, Nucl. Phys. **48**, 652 (1963).<sup>13</sup> R. H. Dalitz, Enrico Fermi Institute for Nuclear Studies, University of Chicago, Report No. 9, 1962 (unpublished).<sup>14</sup> R. H. Dalitz, Enrico Fermi Institute for Nuclear Studies, University of Chicago, Report No. 29, 1963 (unpublished).<sup>15</sup> M. M. Block and R. H. Dalitz, Phys. Rev. Letters **11**, 531 (1963).<sup>16</sup> R. H. Dalitz and G. Rajasekharan, Phys. Letters **1**, 58 (1962).<sup>17</sup> R. H. Dalitz and L. Liu, Phys. Rev. **116**, 1312 (1959).

the  $\Lambda N$  system in an  $s$  state of total spin  $S$ , where

$$\begin{aligned} N &= n \text{ for neutrons} \\ &= p \text{ for protons} \end{aligned}$$

and

$$\begin{aligned} S &= 0 \text{ for singlet interaction} \\ &= 1 \text{ for triplet interaction.} \end{aligned}$$

From Dalitz's theory and the value of  $C_4^7$ ,

$$\frac{R_{n1}}{R_{n0}} = 1.4 \frac{\Gamma_{\pi^-(\Delta\text{He}^5)} Q(\Delta\text{He}^5)}{\Gamma_{\pi^-(\Delta\text{He}^4)} Q(\Delta\text{He}^4)} - 1.8. \quad (3)$$

With the value of  $Q(\Delta\text{He}^4)$ ,<sup>7</sup> and the  $Q(\Delta\text{He}^5)$  value obtained in this work, one gets

$$\frac{R_{n1}}{R_{n0}} = 3.3 \frac{\Gamma_{\pi^-(\Delta\text{He}^5)}}{\Gamma_{\pi^-(\Delta\text{He}^4)}} - 1.8. \quad (4)$$

Absolute values of  $\Gamma_{\pi^-(\Delta\text{He}^4)}$  and  $\Gamma_{\pi^-(\Delta\text{He}^5)}$  are not well known. However, using the completeness-relation method, Dalitz<sup>13,14</sup> showed that the ratio  $[\Gamma_{\pi^-(\Delta\text{He}^5)}] / [\Gamma_{\pi^-(\Delta\text{He}^4)}]$  should be close to unity. Thus, taking  $\Gamma_{\pi^-(\Delta\text{He}^5)} = \Gamma_{\pi^-(\Delta\text{He}^4)}$  one obtains

$$R_{n1} = 1.5 R_{n0}, \quad (5)$$

which implies that the  $\Lambda$ - $n$  force is about 1.5 times stronger in the triplet configuration than in the singlet configuration.

At this point a check can be made to see if this value of  $R_{n1}$  is consistent with the  $\Delta I = \frac{1}{2}$  rule. From this rule

the theory predicts

$$R_{p0} = \frac{1}{2}R_{n0} \quad \text{and} \quad R_{p1} \geq \frac{1}{2}R_{n1}. \quad (6)$$

Using  $R_{p0} = \frac{1}{2}R_{n0}$  and Eq. (5), we obtain

$$R_{p1} = 1.3R_{n0} \quad \text{and hence} \quad R_{p1}/R_{n1} \simeq 0.87,$$

which is certainly greater than 0.5. Hence, the  $\Delta I = \frac{1}{2}$  rule is not violated by our results. Also, if  $\Delta I = \frac{1}{2}$  rule holds,

$$R_{p1}/R_{p0} = 2.6,$$

which implies that the  $\Lambda$ - $p$  force is also stronger in the triplet configuration than in the singlet configuration by a factor of about 2.6 as compared with the factor 1.5 for the  $\Lambda$ - $n$  force.

Furthermore, the value for  $C_5$ , using the above mentioned values of  $C_4$ ,  $Q(\Lambda\text{He}^4)$ , and  $Q(\Lambda\text{He}^5)$ , is given by

$$C_5 = \left[ 2.25 \frac{\Gamma_{\pi^-}(\Lambda\text{He}^5)}{\Gamma_{\pi^-}(\Lambda\text{He}^4)} - 1 \right]^{-1}. \quad (7)$$

Again, making the assumption that

$$\Gamma_{\pi^-}(\Lambda\text{He}^5) = \Gamma_{\pi^-}(\Lambda\text{He}^4),$$

we get

$$C_5 = 0.80.$$

From Table VI it can be seen that this value is not inconsistent with the experimental results and further suggests a cutoff energy for the fast proton of about 25 MeV.

### C. Absolute Decay Rates

In order to get absolute values for the nonmesonic decay rates  $\Gamma_{nm}$ ,  $\Gamma_{\pi^-}(\Lambda\text{He}^4)$  and  $\Gamma_{\pi^-}(\Lambda\text{He}^5)$  must be known. The value of about  $0.25 \Gamma_\Lambda$  given by Dalitz<sup>13,14</sup> for these decay rates seems to be too low when more recent lifetimes are used. The mean lifetime of  $\Lambda\text{He}$  is taken to be  $1.9 \times 10^{-10} \text{ sec}^1$  and the further assumption

made that  $\Gamma(\Lambda\text{He}) = 0.8\Gamma(\Lambda\text{He}^5) + 0.2\Gamma(\Lambda\text{He}^4)$ , as indicated by previous work,<sup>4</sup> where  $\Gamma = \Gamma_{\pi^-} + \Gamma_{nm} + \Gamma_{\pi^0}$ .

Using

$$\Gamma_{nm}(\Lambda\text{He}^5) = 1.21\Gamma_{\pi^-}(\Lambda\text{He}^5) \quad (\text{present work}),$$

$$\Gamma_{\pi^0}(\Lambda\text{He}^5) = 0.50\Gamma_{\pi^-}(\Lambda\text{He}^5) \quad (\text{from } \Delta I = \frac{1}{2} \text{ rule}),$$

$$\Gamma_{nm}(\Lambda\text{He}^4) = 0.52\Gamma_{\pi^-}(\Lambda\text{He}^4) \quad (\text{Ref. 7}),$$

$$\Gamma_{\pi^0}(\Lambda\text{He}^4) = 2.49\Gamma_{\pi^-}(\Lambda\text{He}^4) \quad (\text{Ref. 7}),$$

and

$$\Gamma_\Lambda = 3.98 \times 10^9 \text{ sec}^{-1}$$

for the free  $\Lambda$  particle<sup>6</sup> and again assuming that

$$\Gamma_{\pi^-}(\Lambda\text{He}^5) = \Gamma_{\pi^-}(\Lambda\text{He}^4),$$

the value  $0.44\Gamma_\Lambda$  is obtained for these  $\pi^-$  decay rates.<sup>18</sup>

The nonmesonic and the total decay rates of  $\Lambda\text{He}^4$  and  $\Lambda\text{He}^5$  will then be

$$\Gamma_{nm}(\Lambda\text{He}^4) = 0.23\Gamma_\Lambda,$$

$$\Gamma_{nm}(\Lambda\text{He}^5) = 0.53\Gamma_\Lambda,$$

$$\Gamma(\Lambda\text{He}^4) = 1.21\Gamma_\Lambda,$$

$$\Gamma(\Lambda\text{He}^5) = 1.76\Gamma_\Lambda.$$

### ACKNOWLEDGMENTS

We would like to thank Professor P. L. Jain and Professor W. H. Barkas for assistance in obtaining the exposure at the Bevatron, and Dr. E. F. Lofgren and the Bevatron staff for the exposure to the stopping  $K^-$  beam. We are indebted to Professor P. H. Steinberg for the loan of microscopes. We would also like to thank John Czirr and James Kelly for assistance in carrying out various phases of the experiment. We are grateful for computing time made available to us by the University Computing Center.

<sup>18</sup> These values of the decay rates yield:  $R_{n0} = 11.3\Gamma_\Lambda \text{ F}^3$ ,  $R_{n1} = 17.0\Gamma_\Lambda \text{ F}^3$ ,  $3R_{p1} + R_{p0} = 49.7 \Gamma_\Lambda \text{ F}^3$ , and if the  $\Delta I = \frac{1}{2}$  rule holds,  $R_{p0} = 5.6 \Gamma_\Lambda \text{ F}^3$ ,  $R_{p1} = 14.7 \Gamma_\Lambda \text{ F}^3$ .